LA-UR 91-3605

LA-UR--91-3605

DE92 003852

Los Alamos National Laboratory is operated by the University of California for the United States Department of Energy under contract W-7405-ENG-36

TITLE: SYNTHESIS OF MOLYBDENUM DISILICIDE BY MECHANICAL ALLOYING

AUTHOR(S): R. B. Schwarz
S. R. Srinivasan
J. J. Petrovic
C. J. Maggiore

SUBMITTED TO: First high Temperature Structural Silicides Workshop, NIST, Gaithersburg, MD, November 4-6, 1991; published in Mater. Sci. and Engineering

DISCLAIMER

Los Alamos National Laboratory
Los Alamos, New Mexico 87545

FORM NO. 836 R4
ST. NO. 2629 5/81

SYNTHESIS OF MOLYBDENUM DISILICIDE BY MECHANICAL ALLOYING*

R. B. Schwarz, S. R. Srinivasan, J. J. Petrovic, and C. J. Maggiore
Center for Materials Science
and Materials Science and Technology Division
Los Alamos National Laboratory
Los Alamos, NM 87545

1. INTRODUCTION

The potential and the importance of molybdenum disilicide was realized as early as 1949, evident from the rich body of literature of the time dealing with the synthesis, processing and characterization of this material [1,2]. The combination of high melting point (2050°C), low density (6.24 g cc^{-1}), and extremely high resistance to oxidation and corrosion makes $MoSi_2$ an attractive candidate material for high-temperature structural applications. A review of its properties with particular emphasis on its oxidation and chemical resistance appears in Schlichting [3] and the literature cited therein. The increasing use of $MoSi_2$ as a heating element in furnaces operating in air at temperatures up to 1700°C is a clear demonstration of its excellent high-temperature properties.

The interest to develop $MoSi_2$ as a high-temperature structural material is motivated by the need for materials that can operate at temperatures above 1100°C, the upper limit for Ni-based superalloys [4-9]. However, this proposed development has been slow because $MoSi_2$ is brittle at temperatures below 900°C; MoSi2 undergoes a brittle-to-ductile transition (BDT) at 900°C. Above this temperature $MoSi_2$ becomes ductile [5,6], a behavior that sets it apart from other high-temperature candidate materials such as ceramics and some intermetallics. A disadvantage of the BDT, however, is that the increased ductility leads to a

---

* Paper presented at the *First High Temperature Structural Silicides Workshop*, NIST, Gaithersburg, MD, November 4-6, 1991. Paper to be published in *Mater. Sci. and Engineering*.

concomitant decrease in strength. Current work on $MoSi_2$ is directed towards a simultaneous improvement of the low-temperature ductility and the high-temperature strength. Strength increases are being achieved by solid-solution strengthening with WSi_2, second-phase additions such as Mo_5Si_3 and Ti_5Si_3, [10] and additions of whiskers or ceramic particulates such as SiC and partially stabilized zirconia (PSZ) [8,9,11]. Such attempts have had success at least in identifying the most promising second-phase additions such as PSZ [8-11]. Consequently, the development of $MoSi_2$ as a matrix for ceramic-matrix composites [4,8-11], rather than as a stand-alone high-temperature structural material, appears very promising.

$MoSi_2$ has been synthesized by various methods such as conventional arc-melting and casting, powder pressing and sintering, reaction sintering, and hot-pressing [1,4,12]. There are at least two important considerations in the synthesis and processing of $MoSi_2$. Firstly, the conventional melting route is hampered by the high melting point of $MoSi_2$. Secondly, in all these synthesis methods, oxygen invariably is incorporated in the material during processing. Oxygen reacts with Si to form a glassy SiO_2 second-phase in the $MoSi_2$ matrix [1,4,7,11]. Paradoxically, this silica, when formed at the surface, is responsible for the excellent oxidation and corrosion resistance of $MoSi_2$.

The SiO_2 formed during processing typically segregates to the grain boundaries. The presence of this glassy phase, with a softening temperature close to 1650°C, is detrimental to the high temperature strength and creep properties of $MoSi_2$. Maxwell [1] describes the extensive steps taken during the processing of $MoSi_2$ to reduce the amount of oxygen present as molybdic oxide and silica. These included washing the arc-cast and ground $MoSi_2$ powders in hot, concentrated sodium hydroxide before hot-pressing. Presently, several research groups are involved in synthesizing oxygen-free $MoSi_2$ [13]. There is one view that

intergranular silica particles may help reduce grain growth during high-temperature processing of $MoSi_2$ by pinning the grain boundaries [7]. Nevertheless, the general consensus in the research community is that silica has adverse effects on the high-temperature properties of $MoSi_2$.

We have used mechanical alloying (MA), a high-energy ball-milling process, to prepare $MoSi_2$ and $MoSi_2$-based alloys starting from mixtures of the pure elements. This synthesis route has the potential for preparing oxygen-free $MoSi_2$ and the flexibility for close control of second-phase additions. MA, first developed for producing oxide-dispersions in Ni-based superalloys [14], takes advantage of the atomic-level mixing accomplished by the intense mechanical working of the alloy constituents. All the alloying reactions during the process occur in the solid-state [15,16]. This technique is thus well-suited for synthesizing high melting point materials such as $MoSi_2$. The product of the MA process is a highly homogeneous and fine-grained powder. Its purity is determined by the purity of the starting materials and possible impurities introduced during processing. However, a careful control of the MA process enables a minimization of the impurities.

We also report here the consolidation of the mechanically alloyed powder and the characterization of the $MoSi_2$ alloys by optical and transmission electron microscopy, x-ray diffraction, and mechanical property measurements. We are aware of only two previous studies om the use of MA for the synthesis of silicides of Ti, Fe, Nb, V, and Ta [17,18]. Both these studies are of a preliminary nature and $MoSi_2$ has been reported in passing in only one of these [17], with no mention of consolidation or characterization. In our view, it is essential that this important technique (MA) be used for the synthesis of these promising intermetallic materials to exploit the advantageous features of MA.

2. EXPERIMENTAL

The compositions studied were $MoSi_2$, $MoSi_2$-27 mol% Mo_5Si_3, $MoSi_2$-50 mol% Mo_5Si_3, and $MoSi_2$-50 mol% WSi_2. The MA and all handling of the powders was done inside an argon-filled glovebox. The argon gas is continuously recirculated and has less than 0.1 ppm O_2 and 0.1 ppm H_2O (by volume). The MA was done in a Spex model 8000 laboratory ball-mill located inside the glovebox. We used tungsten carbide-lined stainless steel containers and one 11-mm diameter tungsten carbide ball. The starting powder was a mixture of 99.9% pure, -325 mesh, molybdenum powder, and 99.9999% pure silicon powder. The Si powder was prepared in the same ball-mill starting from Si chunks. The lids of the container were sealed with corprene gaskets. For all the MA runs, the total powder charge was 5 g and the milling time was 20 h. The amount of powder recovered after MA was typically 70% after the first run, and close to 100% for successive runs using the same container and ball. Several MA runs were made to obtain the 40-g batches needed for consolidation and characterization experiments. We detected no change in the weight of the tungsten carbide ball (± 0.01 g) after 30 or more MA runs. This indicated that the contamination of the powder by the milling media was negligible, if any. We detected no tungsten in any of the alloys by energy-dispersive x-ray spectroscopy (EDXS) analysis done in the electron microscope.

The structure of the powders was studied by x-ray diffraction. Before each diffraction run we added a small amount of silicon powder (standard reference material from the National Institute for Standards and Technology, No. SRM640b) to obtain accurate measurements of lattice parameters. We used a Perkin-Elmer 1700 differential thermal analyzer to study phase transformations during the annealing of the powders in high-purity argon. This instrument was calibrated with standard reference materials.

We consolidated the mechanically alloyed powders in graphite dies lined with graphite paper (Grafoil). For the initial tests,

the dies were loaded in air, following the removal of the powder from the glovebox. These powders were hot-pressed within a couple of days. For the latter tests, the dies were loaded inside the glovebox and were transferred to the induction furnace/press inside a plastic bag, also filled with argon gas. These dies were pressed immediately afterward. In spite of this precaution, we expect some seepage of air into the die occurred during the transferring of the die to the induction furnace/press. Table 1 summarizes the processing parameters and the nominal compositions of the alloys studied. The hot-pressing was done at 1500°C and a pressure of approximately 12 MPa for all the alloy powders studied. The die was heated in argon by induction heating and the temperature was monitored by optical pyrometry. The pressure was applied upon reaching 1500°C. This condition of temperature and pressure was kept for 20 minutes. The sample was then slowly cooled under pressure. The hot-pressed compact was 31 mm in diameter and about 6.5 mm in thickness. Its density was determined from its weight and dimensions.

Samples for optical and transmission electron microscopy (TEM) were cut by electro discharge machining (EDM). The optical samples were polished to a 1 μm finish using diamond paste. TEM samples were prepared by mechanical polishing, dimpling, and by ion milling with the sample cooled to 80 K.

Bar samples for high-temperature bend tests, 25 mm in length and 2.5 mm in thickness, were cut from the hot-pressed disks by EDM. The widths of the bars were between 6.4 and 6.8 mm. The bars were cut with the tensile face of the bend bar parallel to the hot-pressing direction. The tensile face was ground to a 30 μm finish using special lapping platens and slurries [19]. The four-point bend tests were done in air using a SiC four-point bend fixture with an inner and outer span of 9.5 and 19 mm, respectively. The samples were deformed in an Instron machine at a crosshead speed of 0.5 mm/min and temperatures of 1200°C and

1400°C. An approximate measure of the yield strength was obtained from the load-displacement curve at 0.05 mm offset from the initial linear portion of the curve. The hardness of the samples were measured on polished surfaces using a Leco macro-hardness tester for various loads ranging from 1 to 30 kg.

3. RESULTS AND DISCUSSION

3.1 Powder Morphology

Figure 1 show a scanning electron micrograph of $MoSi_2$ powder after 20 h of mechanical alloying. The figure shows individual particles and loose agglomerates of these particles. Higher magnification SEM reveals that the particles have sizes of the order of 1 μm.

3.2 X-Ray Diffraction and Calorimetry

Figure 2 shows the x-ray diffraction trace of as-mechanically alloyed MA1 powder (Table 1). The pattern reveals a mixture of pure molybdenum and $MoSi_2$, with no evidence of pure Si. There are also traces of the high-temperature hexagonal $MoSi_2$ phase. Similarly, the diffraction patterns from as-mechanically alloyed MA2 and MA3 powders reveal only pure Mo and $MoSi_2$, with no evidence of the Mo_5Si_3 phase. Finally, the diffraction pattern from as-mechanically alloyed powder MA4 shows Bragg peaks of Mo and W and a disilicide of Mo-W. Thus, for none of the alloys investigated do the phases observed in the as-mechanically alloyed powders agree with the corresponding equilibrium phase diagrams. The presence in the x-ray diffraction patterns of Mo (and W) peaks, together with the absence of Si peaks, suggests that a large amount of Si is in solution in molybdenum and/or in the disilicide phases. This situation does not change on increasing the MA time to 70 h. The equilibrium room-temperature solubility of Si in both Mo and $MoSi_2$ is negligible [20]. These results are not surprising, however, because MA is known to extend the terminal solubilities of interstitial solutes [15].

Thermodynamic equilibrium is established upon annealing the as-mechanically alloyed powders. Figure 3 shows the trace from a scanning differential thermal analysis on as-mechanically alloyed MA1 powder. The first peak, labeled A, results from a reaction in the powder whereas the second peak, labeled B, corresponds to the α-β transformation in a piece of manganese added to the same calorimeter cup to enable us to calibrate the measured transformation enthalpy. Room-temperature X-ray diffraction patterns of powder heated to temperatures just below and above that of peak A show that this peak represents the exothermic reaction of the metastable Mo(Si) and $MoSi_2$ phases produced during MA to form a single-phase $MoSi_2$ alloy powder. The enthalpy of reaction, as measured from the area under peak A, is $\Delta H = 355\ J\ g^{-1}$. Similar DTA traces were obtained for the other alloys studied. In all cases, the temperatures of transformation were between 500 and 600°C. The other reaction enthalpies were 17.25, 107.9, and 118.96 J/g for alloys MA2, MA3, and MA4, respectively.

X-ray diffraction patterns taken on powder heated to 900°C in the calorimeter show the expected equilibrium phases. No remnant Mo, W or Si lines are observed. Figure 4 shows the room temperature x-ray diffraction pattern for the MA4 powder heated to 900°C. We observe only one set of Bragg peaks suggesting that the annealed equimolar mixture of $MoSi_2$ and WSi_2 is a solid solution, as suggested previously [8]. Diffraction patterns from the two-phase $MoSi_2$-Mo_5Si_3 alloys (MA2 and MA3) show only Bragg lines corresponding to these two silicide phases.

From the x-ray diffraction patterns we determined the lattice parameters of the alloy phases in the as-mechanically alloyed and annealed conditions. These results are summarized in Table 2. It is somewhat surprising that the lattice parameters of Mo and $MoSi_2$ in the as-mechanically alloyed powders are close to those of pure Mo and $MoSi_2$. The silicon dissolved in one or both of

these phases appears to have little or no effect on their lattice dimensions.

3.2 Consolidation and Microstructural Characterization

Table 3 gives the hot-pressing temperatures and the density of the bulk alloys obtained. For comparison, the table includes the densities of similar alloys made from commercial alloy powders [10]. The data in Table 3 clearly shows that the compacts made from mechanically alloyed powder have higher densities than those made from commercial powder. Notice further that the hot-pressing temperatures used for the mechanically alloyed powder were approximately 300°C lower than that for the commercial powder. All the other parameters such as compact size, hot-pressing pressure, and heating method were same for both types of powder. We attribute the higher densities of the alloys prepared by the MA route to (a) finer particle size, (b) finer grain size, and (c) a thinner oxide scale on the surface of the powder particles. The fine particle size in the MA powders is apparent in Fig. 1. The grain size of the $MoSi_2$ phase in all the as-mechanically alloyed powders, calculated from the width of the x-ray diffraction peaks, was between 10 and 15 nm.

Figures 5a and b show optical micrographs of polished $MoSi_2$ taken with polarized light. Figure 5a is for alloy MA1 and Fig. 5b for alloy CO1. Alloy CO1 was made by hot-pressing commercial $MoSi_2$ powder from Alfa Products (Ward Hill, MA). The hot-pressing temperatures for these compacts were 1500°C and 1600°C, respectively. The figures shows a larger amount of porosity in the alloy CO1, which agrees with its lower hot-pressed density (Table 3). The grains in the MA1 alloy are between 3 and 10 μm in size, reflecting a grain growth during hot-pressing by almost three orders of magnitude. Grain size of the MA1 alloy is approximately four times smaller than that of the CO1 alloy. This difference is most likely the result of the microstructural scale of the powders and the pressing

temperature. The finer grain size is expected to improve room temperature mechanical properties but reduce high-temperature creep resistance.

The grain size of the MA4 alloy is ≤ 1 μm. The grain size of this alloy in the mechanically alloyed condition is similar to that of pure $MoSi_2$, between 10 and 15 nm. That the grain size in (Mo-W)Si_2 (MA4 alloy) is smaller that in $MoSi_2$ (MA1 alloy) suggests that alloying $MoSi_2$ with WSi_2 causes an overall decrease in the self diffusion rates. This may provide a means to improve the high-temperature creep resistance. Similarly, the two $MoSi_2$-Mo_5Si_3 alloys have finer grain sizes compared to the pure $MoSi_2$.

3.3 Chemical Analysis of Oxygen and Carbon in the Compacts

Since the pioneering work of Maxwell [1] it has been recognized that silica precipitates at the grain boundaries of $MoSi_2$ are detrimental to the high-temperature strength of this alloy. Efforts are now being made at various laboratories to develop processing methods that minimize the amount of intergranular SiO_2 [13]. These studies require a quantitative and reproducible method for measuring the average oxygen contained in the alloy. We have used a nuclear (d,p) reactions to determine the average bulk concentration of oxygen in two of our alloys (MA1 and MA5), as well as in an alloy prepared from commercial $MoSi_2$ powder (CO1). The technique also provided the average bulk concentration of carbon. By a careful choice of the energy window of the detected protons, we measure the oxygen and carbon concentrations at a depth of approximately 2.8 μm. The system was calibrated with an analysis on an Al_2O_3 sample. The oxygen and carbon contents of the samples analyzed thus far are given in Table 1.

3.3 Transmission Electron Microscopy

We used TEM to characterize the alloy microstructures. Figures 6 and 7 are bright field images from alloys MA1 and MA4,

respectively. The reduction in grain size upon alloying $MoSi_2$ and WSi_2 is apparent from the micrographs. Second phase particles are apparent at triple points and grain boundaries in both alloys. Selected area diffraction shows these particles to be amorphous. Energy-dispersive x-ray analysis on these particles shows that they are rich in silicon and oxygen. We take this as conclusive evidence that the particles are glassy SiO_2. Similar SiO_2 intergranular particles are seen in the MA2 and MA3 alloys. The presence of SiO_2 in the glovebox-loaded alloys (MA3, MA4, and MA5) indicates that some oxygen contamination does occur during processing, possibly while placing the dies in the induction furnace/press.

From the viewpoint of mechanical properties it is interesting to know whether the SiO_2 phase wets the grain boundaries, especially for deformations at elevated temperatures. These room-temperature TEM observations, however, cannot answer this question.

Figure 8 is bright field TEM image from the commercial alloy of Fig. 5b. The size of the glassy SiO_2 particle, labeled G, is approximately 2.5 μm in diameter. Silica phases of a similar size have been seen in other alloys produce from commercial powders (see, for example, Fig.5 in ref. 14). The size of the SiO_2 particles seem to scale with the grain size and thus increase with increasing processing temperature.

No special precautions were taken to minimize the oxygen content in the alloys made from commercial powder. Table 1 shows that alloys made from mechanically alloyed powder which was loaded in air (MA1) has approximately half the oxygen content of the commercial alloy CO1. To further decrease the oxygen content we prepared a batch of $MoSi_2$ powder (MA5) which we loaded into dies inside the glovebox. The hot-pressing conditions were similar to those used for the other alloys. Table 1 shows a further reduction in the oxygen content of this alloy by a factor of two. Preliminary TEM observations also show a smaller amount

of glassy SiO_2 particles in the MA5 alloy compared to the MA1 alloy.

3.4 Mechanical Properties

3.4.1 Room Temperature Hardness Measurements

The hardness of the alloys was measured at room temperature at indentation loads between 1 and 30 kg. Fracture toughness values, measured by the indentation crack length measurements, will be presented elsewhere [21]. The hardness was lowest for the MA1 sample, with an average value of 9.6 GPa. Alloys MA2 and MA3 had a hardness of 12.6 GPa and 13.7 GPa respectively. Alloy MA4 was hardest of the four alloys with a value of 13.9 GPa. These hardness values are upperbound values because they were determined from indentations having cracks at the corners.

3.4.2 High Temperature Flexure Tests

The high-temperature mechanical strength of alloys MA1 to MA4 were measured by four-point bend tests at temperatures of 1200°C and 1400°C. We used this technique because we expected these alloys to have limited ductility. We found, however, that the MA alloys are quite ductile for T > 1200°C. The tests were thus stopped after a total deflection between 1.2 and 2 mm. Figure 9 is a plot of the yield strength as a function of temperature. At 1200°C, pure $MoSi_2$ (alloy MA1) has a yield strength of only 26 MPa. This value is approximately a factor of six lower than the yield strength of $MoSi_2$ alloy prepared from commercial powder, reported in [8]. The other MA alloys have higher strengths. Alloy MA4 shows a seven-fold increase in strength at 1200°C over that of alloy MA1. A sharp drop in the strength is noted for all the MA alloys at 1400°C. At this temperature, the yield strength of the MA1 alloy is comparable to that of $MoSi_2$ prepared from commercial powders [8]. The strength of alloys MA2, MA3, and MA4, could not be compared with their commercial counterparts as no values were found in the literature. Nevertheless, it appears

that the smaller grain size of the present MA alloys results in a lower high-temperature strength. The higher strength in the alloys prepared from commercial powders may also result from a higher carbon contnet (Table 1). The data available to date do not allow us to make a correlation between the powder loading environment (air versus glovebox) and the high-temperature strengths. Thus, the role of grain boundary silica particles is also not clear from these tests.

4. CONCLUSIONS

The mechanical alloying route of synthesis of $MoSi_2$-based alloys starting from elemental constituents has a number of interesting features. The alloys produced from mechanically alloyed powders have higher hot-pressed density than those produced from commercial powders processed in air. Interestingly, the enhanced densification is achieved at lower hot-pressing temperatures, an important cost factor during bulk production. This attractive processing feature is accompanied by a lower grain size of the final alloy, which should lead to improved mechanical properties near ambient temperatures. Furthermore, there is the flexibility of increasing the grain sizes by thermal treatments to the levels required to improve properties such as high-creep resistance.

Another important feature of the MA synthesis route is the chemical homogeneity of the alloy. In the $MoSi_2$-WSi_2 alloys, homogeneity is essential for achieving uniform properties. Mixtures of commercial alloy powders of $MoSi_2$ and WSi_2 tend to be non-homogeneously dispersed and result in a non-homogeneous alloy. The synthesis of these alloys by mechanical alloying, however, starts with the mixture of Mo, W and Si powders in the right proportions and the solid-solution is formed in situ by the intimate and simultaneous mixing of all three constituents. Our EDXS measurements in TEM on randomly chosen grains of alloy MA4 indicated the presence of Mo, W and Si in approximately the same

proportions in all the grains. X-ray mapping studies in a scanning TEM are now underway to corroborate these preliminary results.

Room temperature hardness values show improvement with second-phase additions. The solid-solution strengthening of WSi_2 additions appears to be more effective compared to the dispersion strengthening provided by the Mo_5Si_3 particles in the $MoSi_2$-Mo_5Si_3 alloys.

TEM shows amorphous SiO_2 intergranular particles in all our MA alloys. However, handling the powders inside the glovebox appears to be an easy and effective way to reduce the oxygen content by at least a factor of four. This should provide impetus for the ultimate development of silica-free $MoSi_2$-based alloys. Works in progress include the measurement of room temperature indentation fracture toughness (accounting for the crack profiles) and the measurement of elastic moduli as a function of temperature and composition.

ACKNOWLEDGEMENTS

This work was funded by the U.S. Department of Energy, Office of Basic Energy Sciences. The authors thank Dick Hoover for assistance in the hot-pressing of the powders and with the high-temperature mechanical testing.

REFERENCES

1. W. A. Maxwell, National Advisory Committee for Aeronautics, Reports RM E9G01 (1949), RM E52A04 (1952), E52B06 (1952), and E52D09 (1952).

2. L. Brewer, A. W. Searcy, D. H. Templeton, and C. H. Dauben, *J. Am. Ceram. Soc.* 33(10), 291 (1950).

3. J. Schlichting, *High Temperatures-High Pressures*, 10, 241 (1978) (In German); Oak Ridge National Laboratory Report No. ORNL/TR-89-47, 1989 (English Translation).

4. F. D. Gac and J. J. Petrovic, *J. Am. Ceram. Soc.* 68, C-200 (1985).

5. Y. Umakoshi, T. Sakagami, and T. Yamane, *Phil. Mag.* 59(4), 159 (1989).

6. K. Kimura, M. Nakamura, and T. Hirano, *J. Mater. Sci.* 25, 2487 (1990).

7. J. D. Cotton, Y. S. Kim, and M. J. Kaufman, *J. Mater. Sci.* in press, (1991).

8. J. J. Petrovic and R. E. Honnell, *Ceram. Eng. Sci. Proc.* 11, 734 (1990).

9. J. J. Petrovic and R. E. Honnell, *J. Mat. Sci.* 25, 4453 (1990).

10. J. J. Petrovic, R. E. Honnell, and A. K. Vasudevan, *Mater. Res. Soc. Symp. Proc.* 194, 123 (1990).

11. J. J. Petrovic, R. E. Honnell, T. E. Mitchell, R. K. Wade, and K. J. McClellan, *Proc. 15th Ann. Conf. on Composites and Adv. Ceram.*, January 1991, Cocoa Beach, FL. In press (1991).

12. R. D. Grinthal, *J. Electrochem. Soc.* 107(1), 59 (1960).

13. R. M. Aiken, Martin Marietta Research Labs, Baltimore, MD. Private communication (1991).

14. J. S. Benjamin, *Sci. Amer.* 234(5), 40 (1976).

15. R. B. Schwarz and P. Nash, *J. of Metals* 41(1), 27 (1989).

16. R. B. Schwarz and C. C. Koch, *Appl. Phys. Lett.* 49(3), 146 (1986).

17. G. Le Caer, E. Bauer-Grosse, A. Pianelli, E. Bouzy, and P. Matteazzi, *J. Mater. Sci.* 25, 4726 (1990).

18. R. K. Viswanadham, S. K. Mannan, and S. Kumar, *Scripta Metall.* 22, 1011 (1988).

19. D. C. Zipperian, *Am. Ceram. Bull.* 68(6), 1196 (1989).

20. *Binary Alloy Phase Diagrams*, edited by T. B. Massalski, J. L. Murray, L. H. Bennett, and H. Baker (Amer. Soc. for Metals, Metals Park, Ohio), 1986.

21. S. R. Srinivasan and R. B. Schwarz, Los Alamos National Laboratory, unpublished results (1991).

FIGURE CAPTIONS

Fig. 1 Scanning Electron Micrograph of mechanically alloyed $MoSi_2$ powder.

Fig. 2 X-ray diffraction pattern of $MoSi_2$ powder mechanically alloyed for 20 h. Stars = Mo; Circles = $MoSi_2$.

Fig. 3 Differntial thermal analysis of mechanically alloyed powder of nominal composition $MoSi_2$, taken in flowing argon at a heating rate of 20 K min^{-1}.

Fig. 4 X-ray diffraction pattern of $MoSi_2$-50 mol% WSi_2 powder mechanically alloyed for 20 h and heated to 900°C in the calorimeter. All the diffraction peaks are from $(Mo,W)Si_2$.

Fig. 5a Optical micrograph of $MoSi_2$ prepared from mechanically alloyed powder (alloy MA1).

Fig. 5b Optical micrograph of $MoSi_2$ prepared from commercial powder.

Fig. 6 Transmission electron micrograph of $MoSi_2$ alloy prepared from mechanically alloyed powder (alloy MA1).

Fig. 7 Transmission electron micrograph of $MoSi_2$-50 mol% WSi_2 alloy prepared from mechanically alloyed powder (alloy MA4).

Fig. 8 Transmission electron micrograph of $MoSi_2$ alloy prepared from commercial powder (alloy CO1).

Fig. 9 Yield strength of alloys prepared in this study (Table 1) at 1200°C and 1400°C. The strength was deduced from the load-displacement curve for four-point bending tests at a displacement of 0.05 mm from the elastic loading portion of the curve. The curves joining the data point are schematic.

Table 1. Alloy Designation and Compositions of the Alloys Studied.

Alloy Designation	Die Loading Environment	Nominal Composition	Average Oxygen Content (at%)	Average Carbon Content (at%)
CO1	Air	$MoSi_2$	1.11 ± 0.06 (0.118)*	0.69 ± 0.04 (0.055)
MA1	Air	$MoSi_2$	0.61 ± 0.04 (0.064)	0.18 ± 0.02 (0.014)
MA2	Air	$MoSi_2$-27 mol% Mo_5Si_3	-	-
MA3	Glovebox	$MoSi_2$-50 mol% Mo_5Si_3	-	-
MA4	Glovebox	$MoSi_2$-50 mol% WSi_2	-	-
MA5	Glovebox	$MoSi_2$	0.29 ± 0.03 (0.031)	0.18 ± 0.02 (0.014)

* - Numbers in parantheses correspond to equivalent wt%.

Table 2. Lattice Parameters in as-Mechanically Alloyed Powder and Powder Heated to 900°C

MATERIAL	LATTICE PARAMETERS IN nm					
	as-MA Powder			Powder heated to 900°C		
	Phase	a	c	Phase	a	c
$MoSi_2$	$MoSi_2$	0.3203	0.7859	$MoSi_2$	0.3206	0.7860
(MA1)	Mo	0.3147	-	-	-	-
$MoSi_2$-27 mol%Mo_5Si_3	$MoSi_2$	0.3203	0.7865	$MoSi_2$	0.3205	0.7857
(MA2)	Mo	0.3147	-	Mo_5Si_3	0.9639	0.4915
$MoSi_2$-50 mol%Mo_5Si_3	$MoSi_2$	-	-	$MoSi_2$	0.3206	0.7872
(MA3)	Mo	0.3146	-	Mo_5Si_3	0.9641	0.4916
$MoSi_2$-50 mol%WSi_2	$(Mo,W)Si_2$	0.3208	0.7850	$(Mo,W)Si_2$	0.3206	0.7844
(MA4)	Mo/W	0.3160	-	-	-	-

Table 3. Consolidation Temperatures and Densities of Alloys Prepared from Mechanically Alloyed Powders (MA Alloys) and from Commercial Alloy Powders (Commercial Alloys) [10].

MATERIAL	MA ALLOYS			COMMERCIAL ALLOYS		
	Hot-Press Temp (°C)	Final Density (g/cc)	Percent of Theoret.	Hot-Press Temp (°C)	Final Density (g/cc)	Percent of Theoret.
$MoSi_2$	1500	6.02	96.6	1820	5.89	94.5
$MoSi_2$-27 mol%Mo_5Si_3	1500	7.09	97.7	-	-	-
$MoSi_2$-50 mol%Mo_5Si_3	1500	7.49	97.0	1810	7.44	96.4
$MoSi_2$-50 mol%WSi_2	1500	7.65	96.8	1820	7.37	93.3

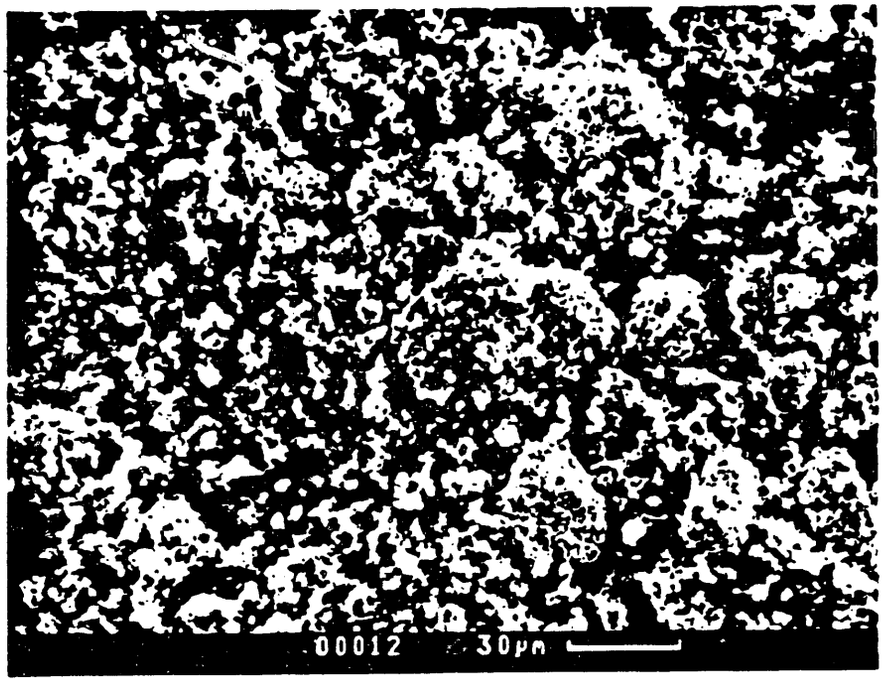

Fig. 1 Scanning Electron Micrograph of mechanically alloyed $MoSi_2$ powder.

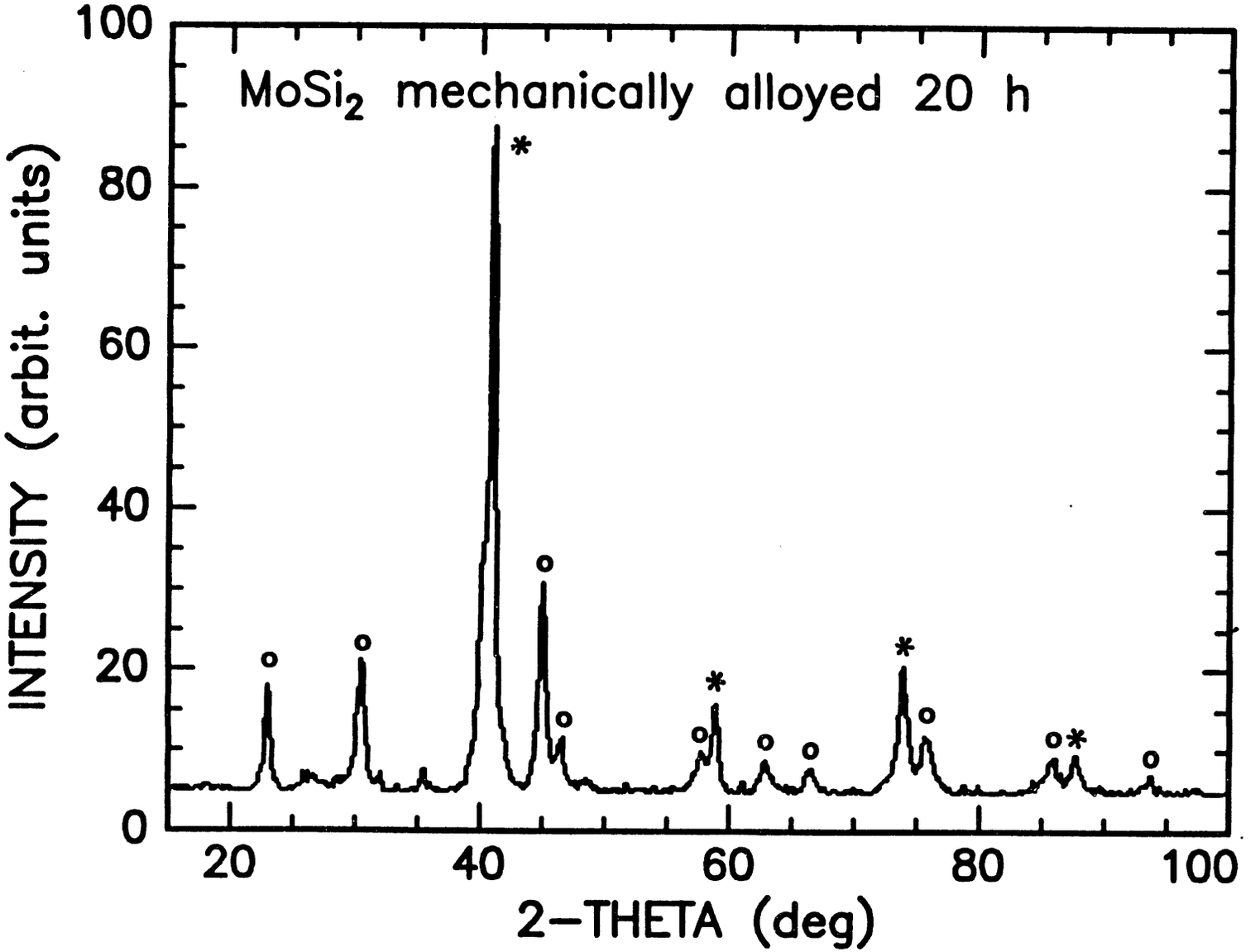
MoSi2 mechanically alloyed 20 h
INTENSITY (arbit. units)
2-THETA (deg)
0
20
40
60
80
100
20
40
60
80
100

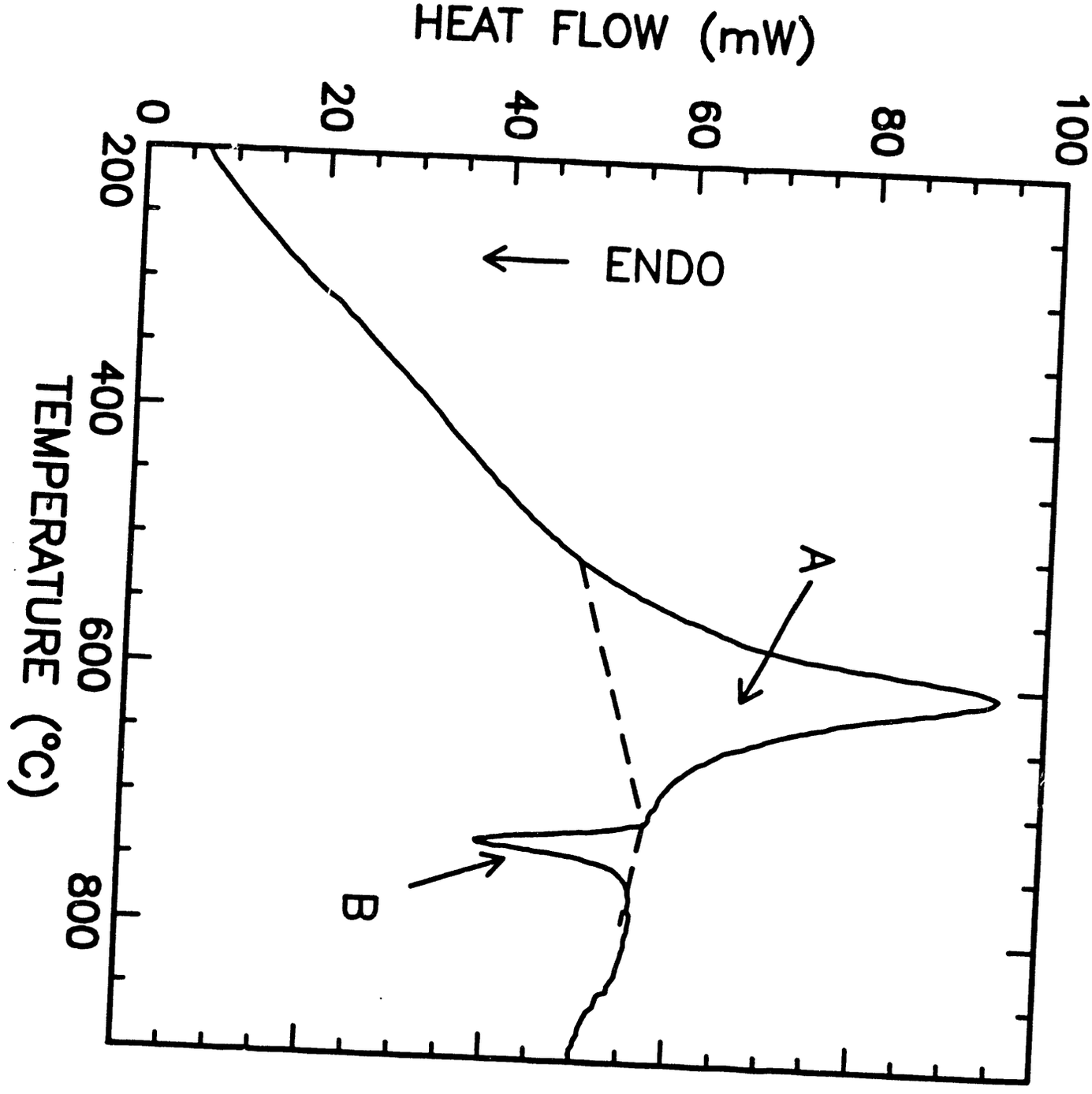
HEAT FLOW (mW)
0
20
40
60
80
100
200
400
600
800
TEMPERATURE (°C)
ENDO
A
B

Fig. 3

Fig. 4

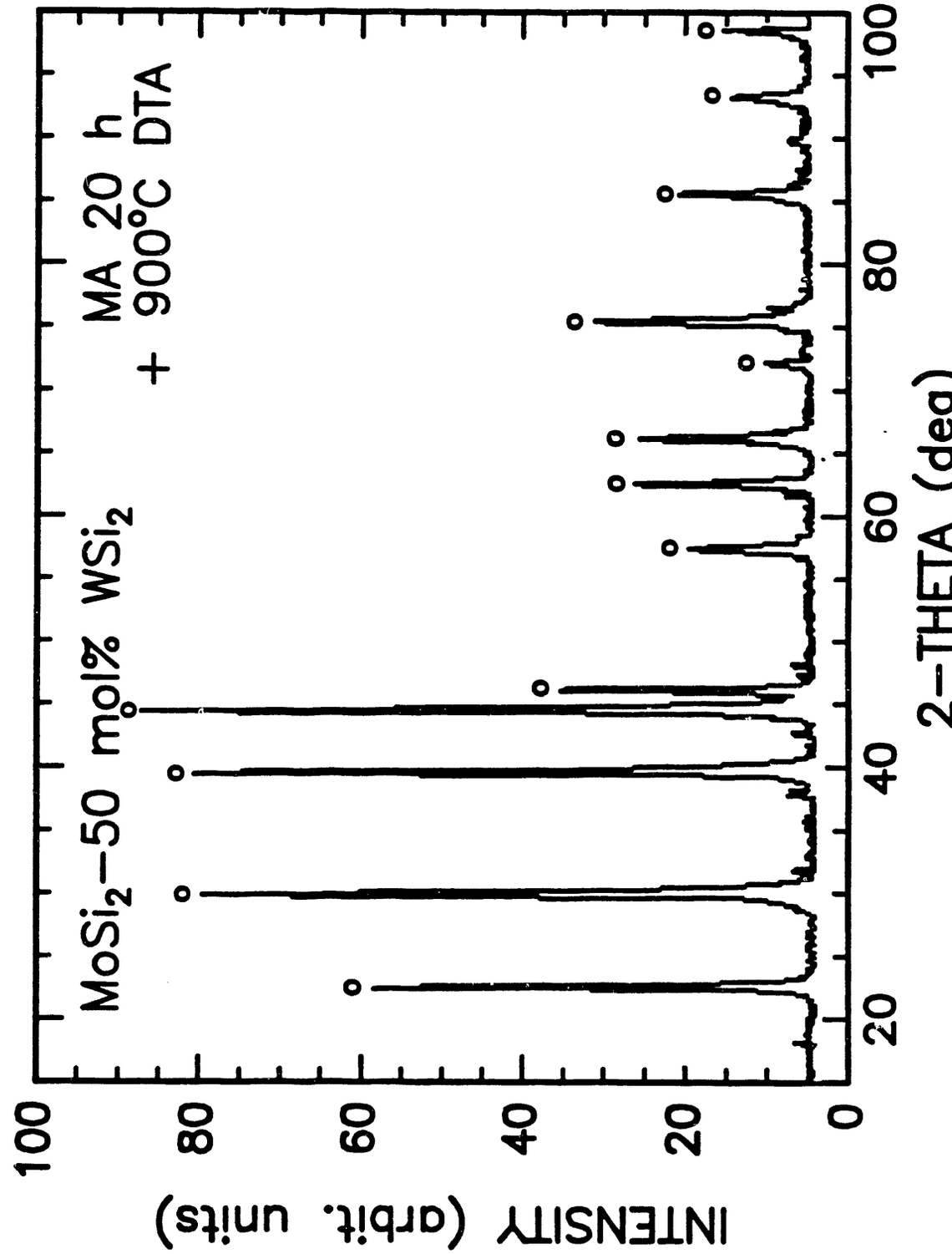
MoSi2–50 mol% WSi2
MA 20 h
+ 900°C DTA
INTENSITY (arbit. units)
2–THETA (deg)
0
20
40
60
80
100
20
40
60
80
100

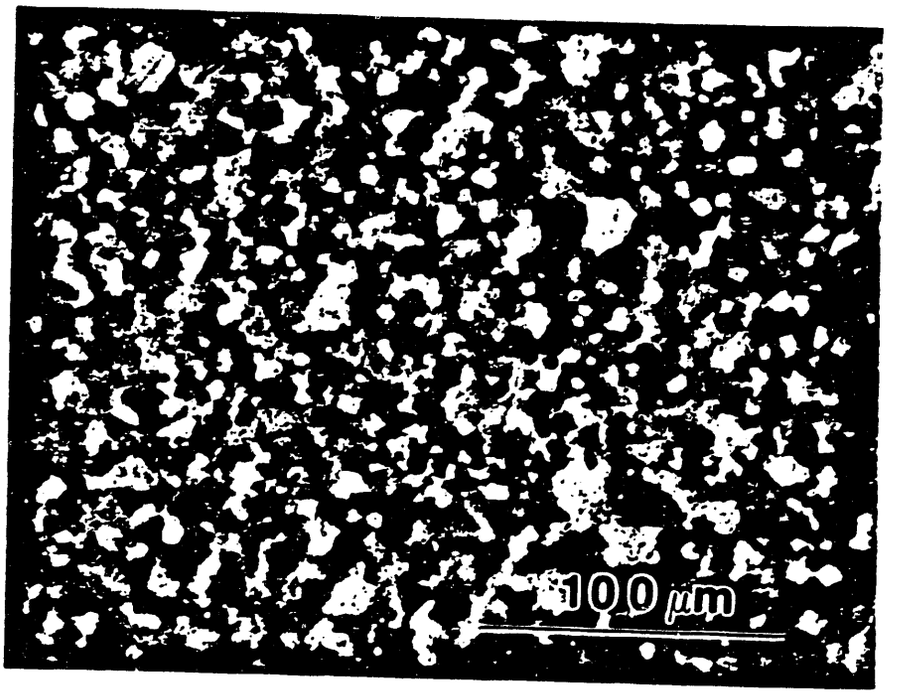

Fig. 5a Optical micrograph of $MoSi_2$ prepared from mechanically alloyed powder (alloy MA1).

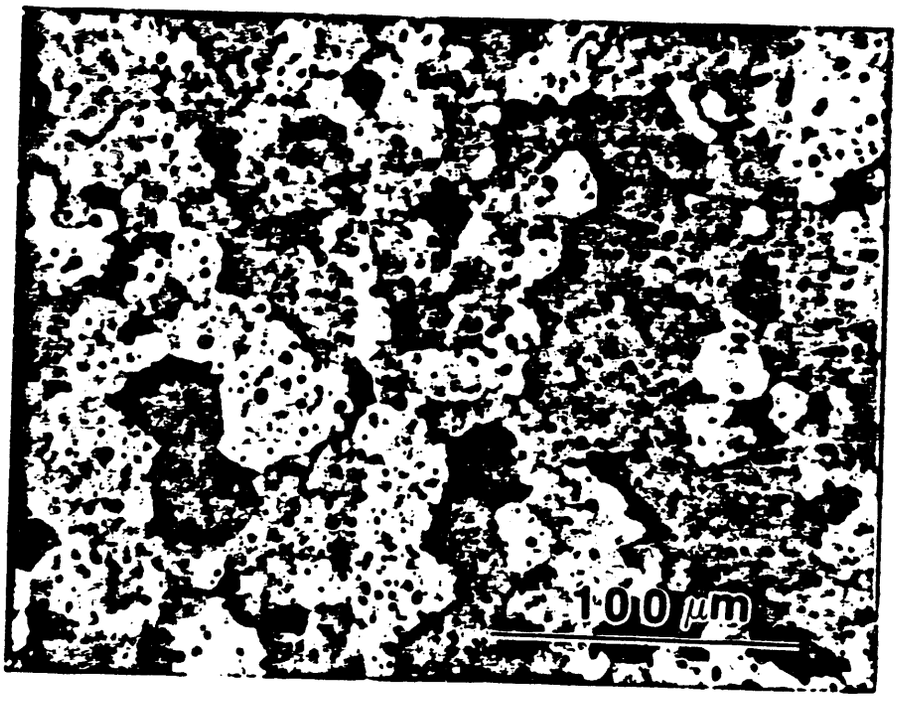

Fig. 5b Optical micrograph of $MoSi_2$ prepared from commercial powder.


130KP.8.2.8.
1 µm

fig. 7

Fig 8

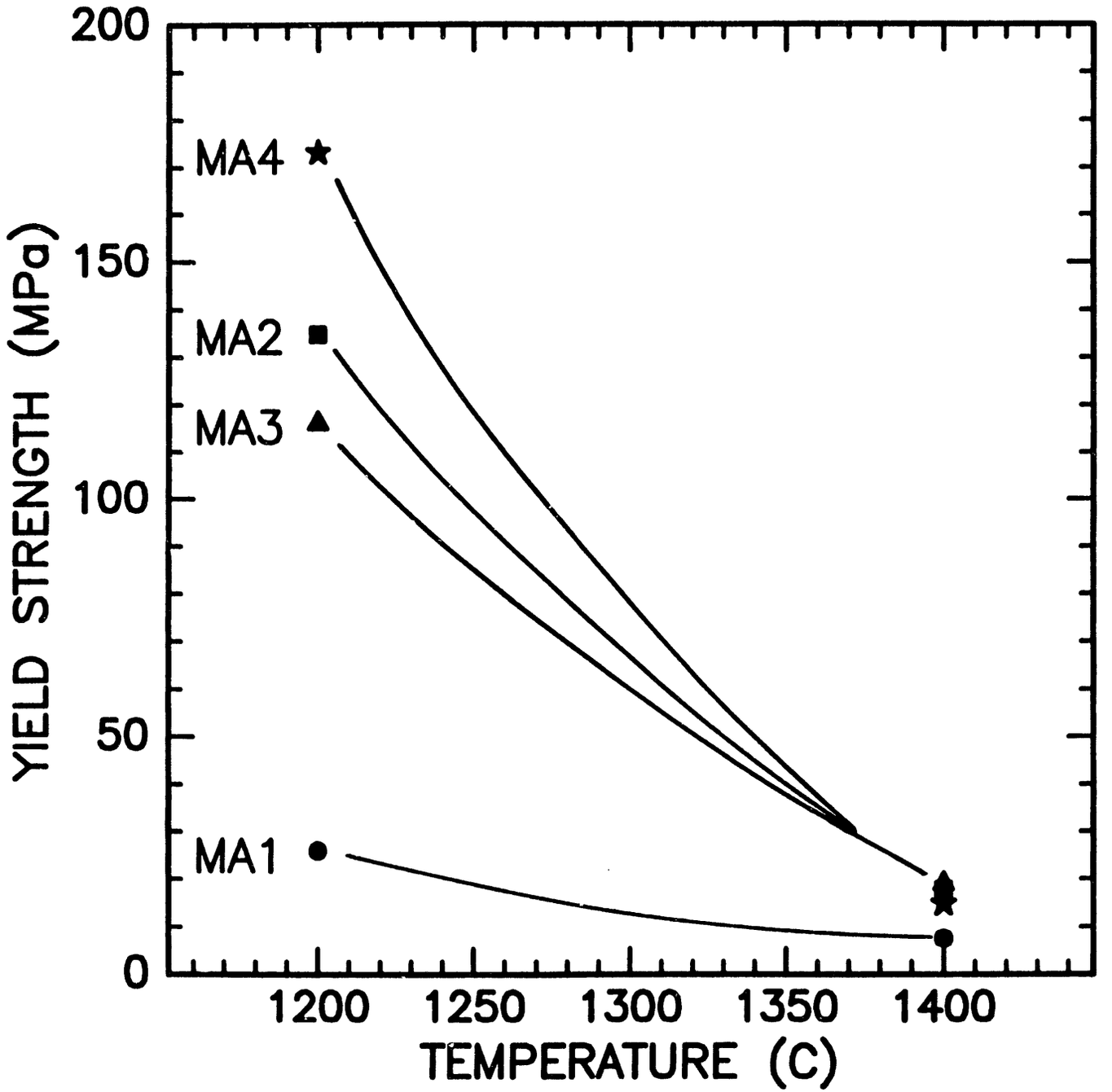
200
150
100
50
0
YIELD STRENGTH (MPa)
MA4
MA2
MA3
MA1
1200
1250
1300
1350
1400
TEMPERATURE (C)

Fig. 9

END

DATE FILMED

01/06/92